A&A 437, 447–456 (2005)
DOI: 10.1051/0004-6361:20042442

Astronomy & Astrophysics

Is the Galactic submillimeter dust emissivity underestimated?

K. M. Dasyra[1,2], E. M. Xilouris[3], A. Misiriotis[2], and N. D. Kylafis[2,4]

[1] Max-Planck-Institut für Extraterrestrische Physik, Postfach 1312, 85741 Garching, Germany
e-mail: dasyra@mpe.mpg.de
[2] University of Crete, Physics Department, PO Box 2208, 71003 Heraklion, Crete, Greece
[3] National Observatory of Athens, I. Metaxa & Vas. Pavlou str., Palaia Penteli, 15236 Athens, Greece
[4] Foundation for Research and Technology-Hellas, PO Box 1527, 71110 Heraklion, Crete, Greece

Received 26 November 2004 / Accepted 9 March 2005

Abstract. We present detailed modeling of the spectral energy distribution (SED) of the spiral galaxies NGC 891, NGC 4013 and NGC 5907 in the far-infrared (FIR) and sub-millimeter (submm) wavelengths. The model takes into account the emission of the diffuse dust component, which is heated by the UV and optical radiation field produced by the stars, as well as the emission produced locally in star forming HII complexes. Radiative transfer simulations in the optical bands are used to constrain the stellar and dust geometrical parameters and the dust mass. We find that the submm emission predicted by our model cannot account for the observed fluxes at these wavelengths. Two scenarios that could account for the "missing" submm flux are examined. In the first scenario dust additional to that derived from the optical wavelengths is embedded in the galaxy in the form of a thin disk. This additional dust disk, which is not detectable in the optical and which is associated with the young stellar population, gives rise to additional submm emission, and makes the total flux match the observed values. The other scenario examines the possibility that the average emissivity at submm wavelengths of the dust grains found both in a diffuse component and in denser environments (e.g. molecular gas clouds) is higher than the values widely used in Galactic environments. This enhanced emissivity reproduces the observed FIR and submm fluxes with the dust mass equal to that derived from the optical observations. In the second scenario, we treat the submm emissivity as a free parameter and calculate its nominal value by fitting our model to the observed SED. We find a dust emissivity which is ~3 times the often-used values for our Galaxy. Both scenarios can equally well reproduce the observed 850 μm surface brightness for all three galaxies. However, we argue that the scenario of having more dust embedded in a second disk is not supported by the near infrared observations. At 2.16 μm, the model images with a second dust disk reveal a prominent dust lane which is not present in the observations. Thus, the enhanced emissivity at submm wavelengths is a real possibility and the Galactic submillimeter dust emissivity may be underestimated.

Key words. ISM: dust, extinction – galaxies: ISM – galaxies: spiral – infrared: galaxies – submillimeter

1. Introduction

Edge-on spiral galaxies constitute a benchmark for multi-wavelength modeling of the dust content and the properties of dust grains in spiral galaxies. Their unique orientation allows for a direct detection of the dust distribution seen in absorption at optical wavelengths and in emission in the far infrared (FIR) and submillimeter (submm) part of the spectrum. Realistic three dimensional radiative transfer (RT) modeling that was applied to a number of nearby edge-on spiral galaxies (Xilouris et al. 1997, 1998, 1999) has been able to determine the stellar and dust parameters that best fit the optical surface brightness of these galaxies. According to these simulations, a typical spiral galaxy contains $\sim 10^7$ $M_\odot$ of dust grain material distributed in an exponential disk with a scaleheight about half that of the stars and a scalelength about 1.5 times the stellar one. Furthermore, the extinction law at optical and near infrared (NIR) wavelengths calculated for these galaxies matches very well the extinction law observed for our Galaxy, indicating common dust properties among spiral galaxies. The optical thickness of the galactic disk, parameterized by the central face-on optical depth, has values of the order of unity in the B-band.

Complementary to the optical modeling, studies of the FIR emission of edge-on spiral galaxies have also been carried out. In the studies of Popescu et al. (2000), Bianchi et al. (2000), Misiriotis et al. (2001), the FIR/submm energy output of a spiral galaxy is determined by equating it with the energy the dust grains absorb from the UV and optical photons. Popescu et al. (2000) found that their RT model submm fluxes were significantly lower than the observed values. In order to overcome this problem and explain the FIR/submm spectral energy distribution (SED) of spirals, Popescu et al. (2000) used a second dust disk, with scaleheight matching that of the young stellar population found in our Galaxy. However, recent studies question the validity of the values that have been widely

used so far for the FIR/submm emissivity of the dust grains. In particular, a wide range of values (of an order of magnitude) are used for the submm emissivity (see Alton et al. 2004 and Hughes et al. 1997 for reviews of the emissivity values found in the literature). In del Burgo et al. (2003), the FIR properties of dust in high-latitude regions are examined using ISOPHOT maps and an enhancement (about four times) of the emissivity of the big grains with respect to those in the diffuse interstellar medium is indicated. In the study of Alton et al. (1998) and in a more recent study (Alton et al. 2004), the submm emissivity was calculated for the edge-on galaxies NGC 891, NGC 4013 and NGC 5907 by comparing the distribution of their visual optical depth with their 850 μm emission. This analysis produced an emissivity at 850 μm which is about four times the widely adopted value of Draine & Lee (1984). Alton et al. (2004) argue that since the submm emission closely follows the distribution of molecular gas, the relatively high emissivity values might be due to dust situated mainly in molecular gas clouds where the enhanced density is conducive to formation of amorphous, fluffy grains. Such grains are expected to possess high emissivity values. In a recent study of the large-scale variations of the dust optical properties in the Galaxy (Cambrésy et al. 2005), the authors suggest that this type of dust grain is more common than previously thought since they would be formed even at low extinction and not only in dense cold clouds.

In this paper we use a three dimensional model of the emission of the dust grains in order to fit the FIR/submm SED of three edge-on spiral galaxies (NGC 891, NGC 5907, and NGC 4013) already modeled in the optical wavelengths by Xilouris et al. (1999). Two different scenarios concerning the dust properties are examined. In the first scenario (hereafter "1-disk" model) the dust is distributed in a single exponential disk (that derived by Xilouris et al. 1999) with the FIR/submm emissivity treated as a free parameter so that the model SED matches the observed one. In the second case (hereafter "2-disk" model) an additional dust disk of smaller scaleheight with respect to the main dust disk is invoked. This disk is associated with the young stellar population and it contains, like the main disk, dust grain material with properties as described in Draine (2003). The sum of the two dust disks then gives rise to the FIR/submm flux that matches the observed SED. We show that both of these models are able to reproduce the observed surface brightness at 850 μm. The "2-disk" model is tested for consistency by comparing the model K-band image with the observed one. The model K-band image exhibits a prominent dust lane which is not seen in the observations. From this test we conclude that the additional dust, if such is needed, cannot be in the form of a second dust disk. We cannot exclude the possibility that some dust is in the form of clumps. An upper limit for the amount of dust that can be located there has been placed by Misiriotis & Bianchi (2002).

This paper is arranged as follows: In Sect. 2 a description of our model is given. In Sects. 3 and 4 the resulting SEDs of the "1-disk" and "2-disk" models are presented and evaluated. A comparison between the two models is made in Sect. 5 while possible sources of uncertainty are enumerated and discussed in Sect. 6. Finally, our work is summarized in Sect. 7.

2. Model

2.1. General description

The procedure that we follow to create a galactic FIR/submm spectrum is along the lines of Popescu et al. (2000) and is briefly presented here. Our first task is to find the radiation field in which the grains are immersed and from which they draw energy. For this reason we perform RT calculations for every point in the galaxy and for all directions. These calculations need to be performed in all the wavelength regimes where light extinction by dust grains is taking place; namely, in the UV, optical and NIR. Considering that the extinction properties of the dust in these regimes are well-known (Draine 2003), the RT calculations accurately provide us the power that the grains absorb per unit galactic volume. By adopting an appropriate thermal emission law, equating the absorbed with the emitted power per unit volume, and assuming thermal equilibrium we are able to calculate the temperature distribution of the dust $T(r, z)$, where r is the radial direction and z is the direction perpendicular to the galactic plane. Knowing the temperature distribution, we obtain the FIR/submm SED by integrating the emitted power $w_{\rm em}(\lambda, T)$ over the entire galactic volume and converting it into an observable flux. The creation of such a model needs a priori assumptions of the way that the galactic stellar and dust components are distributed as well as the FIR/submm dust emission law.

2.2. Stellar and dust distributions

The geometry of the different components (stellar and dust) of the galaxies examined in this study is based on the analysis of Xilouris et al. (1999), that simulates very accurately the optical images of these galaxies. The actual model that we use is briefly described below.

The old stellar population is distributed in an exponential disk as well as a de Vaucouleurs (1953) bulge. In addition, a young stellar population is used as the main UV heating source of the dust grains. This component is distributed in a thin exponential disk in the galactic plane with the same scalelength as that of the old stellar population and a scaleheight of 90 pc as indicated by studies of the Galactic stellar population (Mihalas & Binney 1981). Quantitatively, the emission coefficients of a stellar disk and a de Vaucouleurs (1953) bulge, $\eta_{\rm s}$ and $\eta_{\rm b}$ respectively, at a galactic position (r, z) and wavelength λ are

$$\eta_{\rm s}(\lambda, r, z) = \eta_{\rm s}(\lambda, 0, 0)\, {\rm e}^{-r/r_{\rm s}}\, {\rm e}^{-|z|/z_{\rm s}}, \quad (1)$$

$$\eta_{\rm b}(\lambda, r, z) = \eta_{\rm b}(\lambda, 0, 0) B^{-7/8}\, {\rm e}^{-7.67 B^{1/4}}. \quad (2)$$

In Eq. (1), $r_{\rm s}$ and $z_{\rm s}$ give the scalelength and scaleheight of a stellar disk respectively. In Eq. (2), $B = \sqrt{r^2 + z^2(a/b)^2}/r_{\rm e}$ and depends on the effective radius $r_{\rm e}$ and the major and minor semi-axes a, b of the bulge.

The dust distribution within the galaxy is described by the extinction coefficient, which is thought to obey the exponential law

$$k_{\rm ext}(\lambda, r, z) = k_{\rm ext}(\lambda, 0, 0)\, {\rm e}^{-r/r_{\rm d}}\, {\rm e}^{-|z|/z_{\rm d}}. \quad (3)$$

The quantities r_d and z_d are the scalelength and the scaleheight of the dust respectively. The central optical depth of the model galaxy seen edge-on is given by $\tau^e = 2k_{ext}(\lambda, 0, 0)r_d$ (Xilouris et al. 1997). In addition to this "main" dust disk, which is derived by modeling the optical appearance of edge-on galaxies (Xilouris et al. 1999), in the case of our "2-disk" model, we use a second thinner dust disk of the same scalelength as that of the "main" dust disk and a scaleheight of 90 pc since this dust is assumed to be associated with the young stellar population (see above).

The opacity (mass extinction coefficient), $\kappa_{ext}(\lambda)$ is defined as $\kappa_{ext}(\lambda) \equiv k_{ext}(\lambda, r, z)/\rho_d(r, z)$, with $\rho_d(r, z)$ being the density of the dust grain material inside the galaxy. It is connected to the mass absorption coefficient as $\kappa_{abs}(\lambda) = (1 - \omega)\kappa_{ext}(\lambda)$, where ω is the scattering albedo. Taking into account that $\kappa_{abs}(\lambda) = \kappa_{em}(\lambda)$ for $\lambda \gg \alpha$ where α is the radius of a typical dust grain (i.e. in the FIR and submm wavelengths), we derive that the mass emission coefficient (a grain's emission cross section over its mass) is $\kappa_{em}(\lambda) = (1 - \omega)\kappa_{ext}(\lambda)$. Additionally to the mass emission coefficient we can define the dust grain emissivity as $Q(\lambda) = (4/3)\alpha\rho\kappa_{em}(\lambda)$ (Whittet 1992), where ρ is the material density of the interstellar grains.

We use the values of Xilouris et al. (1999) for all the quantities that can be inferred from an optical/NIR modeling of the galaxies. These are: $\eta_s(\lambda, 0, 0), \eta_b(\lambda, 0, 0), k_{ext}(\lambda, 0, 0)$ (for λ in the optical/NIR waveband), $r_s, z_s, r_e, a/b, r_d, z_d$, and the inclination angle of each galaxy.

We parameterize the UV luminosity L_{UV} of a spiral galaxy using the star formation rate (SFR) in $M_\odot\,\mathrm{yr}^{-1}$. For this, we use the formula of Kennicutt (1998) as described in Popescu et al. (2000). However, the UV luminosity that heats the diffuse dust in a galaxy is less than that provided by the above equations for a given SFR. The reason is that a non-negligible fraction F of L_{UV} cannot be radiated away from the young stars due to heavy obscuration of certain sightlines by the surrounding HII regions (Popescu et al. 2000). Thus, the fraction of L_{UV} that is available to be absorbed by the diffuse dust is $1 - F$. We add the HII region contribution to the SED of the diffuse dust by using the spectrum of the Galactic region G45.12+0.13 (Chini et al. 1986) as a template and normalizing its luminosity to FL_{UV}.

2.3. FIR/submm emission law

Having identified all the ingredients of our model and formulated their distributions, we still have to assume a dust FIR/submm emission law in order to find the SED, as mentioned in Sect. 2.1.

The selection of the appropriate values for the dust emission coefficient is a major decision in our modeling. As we will soon demonstrate, all the emission coefficients that have been found so far for the diffuse dust of the Milky Way fail to explain the FIR/submm SED of the galaxies in our sample, if we assume that the amount of dust derived from the optical images is correct. This leads us to investigate other ways that can produce the observed SED.

We begin by using the values that Draine (2003) proposes for the Milky Way. These values were calculated by taking into account a mixture of graphites, silicates, and polycyclic aromatic hydrocarbon molecules (PAHs), as well as a distribution of grain sizes (Weingartner & Draine 2001). In particular, we use the tabulated, more detailed data of the website cited in Draine (2003). Several values of κ_{em} found for different grain abundances relative to H are available and described as a function of R_V. According to Draine, the quantity $R_V \equiv A_V/(A_B - A_V)$ shows how steep the slope of the extinction A_λ is in the optical waveband. The extinction is expressed in terms of the flux F_λ as $A_\lambda = 2.5 \log_{10}(F_\lambda^{\mathrm{observed}}/F_\lambda^{\mathrm{unextinguished}})$. We use the cases $R_V = 3.1$ and $R_V = 5.5$. The $R_V = 3.1$ model is considered representative of the mean Galactic obscuration (Whittet 1992), while the $R_V = 5.5$ case roughly agrees with the mid-infrared extinction law at ~5 μm, as observed by Lutz et al. (1996) in the Galactic center direction.

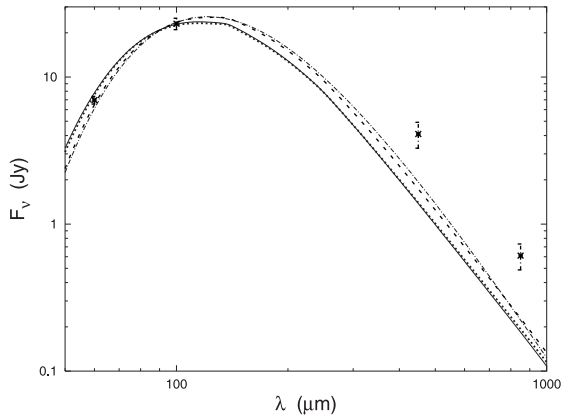

Fig. 1. SED modeling of NGC 4013 using different emission laws. The solid and the dotted lines are derived with the emissivity described in Draine (2003) for $R_V = 3.1$ and $R_V = 5.5$ respectively. The dashed-dotted line is the SED that we derive with the use of the model of Bianchi et al. (1999), and the short-dashed line is the SED produced with the Weingartner & Draine (2001) model for $R_V = 3.1$. In all the cases we have set $SFR = 1.8\ M_\odot\,\mathrm{yr}^{-1}$, and $F = 0$, since we are interested only in the behavior of the diffuse dust.

The emitted power per galactic unit volume and Å, w_{em}, is equal to the flux of the (gray-body) radiation through each grain's spherical surface, times the emitting surface, times the number density of the grains. When we combine the above with the definition of the mass emission coefficient we obtain the following emission law

$$w_{em}(\lambda, T) = 4\pi\rho_d\,\kappa_{em}(\lambda)\,B(\lambda, T), \quad (4)$$

where $B(\lambda, T)$ is the Planck function and T is the temperature of the dust. As already mentioned, we equate the integral of Eq. (4) to the absorbed energy per unit volume to find the temperature of the dust grains. Then, having the T distribution in the galaxy, we return to Eq. (4) to calculate the emitted power as a function of λ.

In Fig. 1 we show as a solid line the SED for NGC 4013 produced with Draine's (2003) emissivity, $SFR = 1.8\ M_\odot\,\mathrm{yr}^{-1}$, $F = 0$, and $R_V = 3.1$. The value of SFR was chosen so that we obtain a good fit to the 60 and 100 μm data (see Sect. 3). The dotted line is the same as the solid one but for $SFR = 1.8\ M_\odot\,\mathrm{yr}^{-1}$, $F = 0$, and $R_V = 5.5$. The reason we

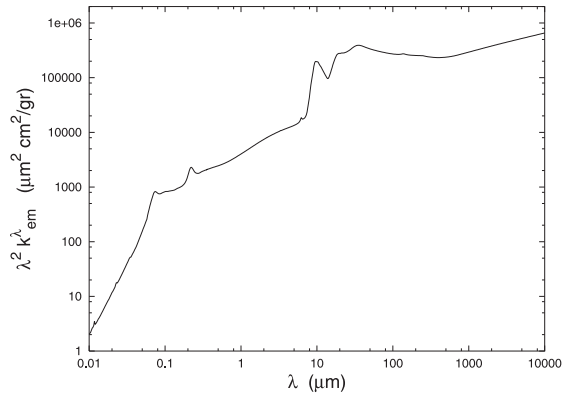

Fig. 2. The Draine (2003) emission coefficient times λ^2 for $R_V = 3.1$. The curve is nearly flat in the regime of our concern ($50 < \lambda < 1500\ \mu$m).

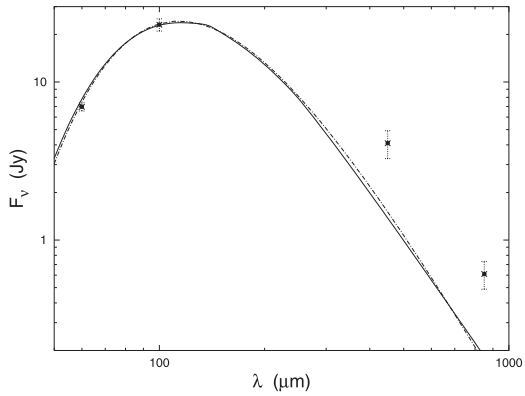

Fig. 3. Same as Fig. 1. The dashed-dotted line is the SED derived from our model with $SFR = 1.8\ M_\odot\,\mathrm{yr}^{-1}$, $F = 0$, and $C_0 = 987$. The solid line is identical to that of Fig. 1.

set $F = 0$ at this point is to compare several emission models that apply only to the diffuse dust. Any conclusion for the submm emissivity derived from this comparison will not be changed with the addition of the HII regions' emission, because it mainly contributes at the FIR wavelengths (see Popescu et al. 2000). Clearly, if we have included in our modeling all the dust that exists in NGC 4013, these emissivity models cannot account for the galaxy's submm SED.

We reach the same conclusion when we use emissivity laws found by other authors. The dashed-dotted line in Fig. 1 is the SED that we derive with the use of the model of Bianchi et al. (1999). This model uses larger (and therefore colder) grains than Draine (2003), $SFR = 1.8\ M_\odot\,\mathrm{yr}^{-1}$, and $F = 0$. The dashed line is the SED produced with the Weingartner & Draine (2001) model for $R_V = 3.1$, $SFR = 1.8\ M_\odot\,\mathrm{yr}^{-1}$, and $F = 0$. In all cases, the observed flux at 450 and 850 μm is significantly higher than the above models. Similar results were reported by Popescu et al. (2000) and Misiriotis et al. (2001).

The approach of Bianchi et al. (1999) in deriving the emissivity is conceptually simpler than that of the other authors, but still trustworthy. Bianchi et al. (1999) used a model that is independent of grain size and composition and that does not take into account the PAH emission in order to explain the FIR flux maps of the Galactic hemispheres. The wavelength dependence of the emission coefficient, as inferred from that study, has the form

$$\kappa_{\rm em}(\lambda) = \frac{\kappa_{\rm ext}(V)}{760}\left(\frac{100\ \mu\mathrm{m}}{\lambda}\right)^2, \tag{5}$$

with $\kappa_{\rm ext}(V)$ being the V band opacity.

Driven by the fact that even the most sophisticated models do not differ much from a $1/\lambda^2$ law in the range $50 < \lambda < 1500\,\mu$m (see Fig. 2), we adopt the Bianchi et al. (1999) assumptions of grains of an average size and composition, that are gray-body emitters. We consider the emission coefficient to be

$$\kappa_{\rm em}(\lambda) = \frac{\kappa_{\rm ext}(V)}{C_0}\left(\frac{100\ \mu\mathrm{m}}{\lambda}\right)^\beta, \tag{6}$$

where $\beta = 2$, C_0 is a parameter to be determined, and $\kappa_{\rm ext}(V) = 2.52\times10^4\ \mathrm{cm}^2\ \mathrm{gr}^{-1}$ (Draine 2003, $R_V = 3.1$). Thus, the parameters in our "1-disk" model are SFR, F, and C_0.

These assumptions lead to the gray-body emission form that we adopt, namely

$$w_{\rm em}(\lambda, T) = 4\pi\frac{\rho_{\rm d}\kappa_{\rm ext}(V)}{C_0}\left(\frac{100\,\mu\mathrm{m}}{\lambda}\right)^\beta B(\lambda, T), \tag{7}$$

with $\beta = 2$. In Sect. 6 we will examine other values of β to see how sensitive our conclusions are to such changes. Furthermore, we will comment there on the effects of the PAHs and the transiently heated, very small grains (VSG), which we did not take into account in our modeling.

What SED would our model give for NGC 4013 in comparison to those shown in Fig. 1? In Fig. 3 we show as a dashed-dotted line the SED produced with our model for $SFR = 1.8\ M_\odot\,\mathrm{yr}^{-1}$, $F = 0$, and $C_0 = 987$. It is remarkably close to the solid line, which is identical to the solid line of Fig. 1. This means that a simple model with the appropriate $\kappa_{\rm em}$ (i.e. appropriate grain size and composition) can mimic a more complicated model and justifies our selection.

2.4. The "2-disk" model

For our "2-disk" model, we keep the stellar disks (old and young) the same as in our "1-disk" model. The dust, however, is now distributed in two disks. One, with mass $M_{\rm d1}$, is identical to that of our "1-disk" model. The second, with mass $M_{\rm d2}$ to be determined, has scalelength $r_{\rm d}$ equal to that of the first disk. Its scaleheight $z_{\rm d}$ is taken equal to 90 pc, as in Popescu et al. (2000). As these authors explain, the second dust disk must have a small scaleheight to be undetected in the optical bands. This is true, at least for wavelengths less than $\sim1\ \mu$m, because the "main" dust disk highly obscures any other feature (the second dust disk included) which is close to the galactic plane. The specific value of 90 pc was used by Popescu et al. (2000) because they associated the second dust disk with the molecular cloud distribution in the Milky way and proposed that it has to be connected with the young stellar population. The addition of the second disk obviously leads to an increase of the central extinction coefficient of Eq. (3). Another difference to the "1-disk" model is that the FIR/submm emissivity is taken from Draine (2003). The free parameters of the "2-disk" model are then SFR, F, and $M_{\rm d2}$.

Table 1. The best fitting parameters for our "1-disk" model.

Galaxy	SFR ($M_\odot$ yr^{-1})	F	C_0
NGC 891	5.80	0.28	330
NGC 4013	1.80	0.17	187
NGC 5907	4.10	0.16	236

3. Results of the "1-disk" model

Following the procedure described in Sect. 2, we determined the parameters that best fit the observational data in the FIR/submm waveband. Their values are given in Table 1 for the three galaxies of our sample.

In Fig. 4 we show our computed SEDs that best fit the observational data. For NGC 891 the observed fluxes are taken from Dupac et al. (2003a), with the exception of the ISO and the IRAM measurements which are taken from Popescu et al. (2004) and Guélin et al. (1993) respectively. For NGC 4013 and NGC 5907 the IRAS data are taken from Soifer et al. (1989) while the SCUBA data are presented in Alton et al. (2004). The 1.2 mm flux of NGC 5907 is reported in Dumke et al. (1997). The short-dashed lines give the contribution to the SEDs of the HII regions, the dashed-dotted lines give the contribution of the diffuse dust and the solid lines represent the total computed SEDs. It is evident that our model SEDs fit very well the observational data.

It is also evident from Table 1 that the average value of our parameter C_0 is 251 and corresponds to $\kappa_{\rm em}(850\ \mu{\rm m}) = 1.4\ {\rm cm^2\ gr^{-1}}$, when using $\kappa_{\rm ext}(V) = 2.52 \times 10^4\ {\rm cm^2\ gr^{-1}}$, as the Draine 2003, $R_V = 3.1$ model prescribes. In Table 2, we compare for each galaxy the 850 μm emission coefficient that we find (from Eq. (6)) to values used in Galactic emission studies. More specifically, we present the ratios $x_{\rm B}$, $x_{\rm W}$, and $x_{\rm D}$ of our 850 μm value to those of Bianchi et al. (1999), Weingartner & Draine (2001), and Draine (2003) respectively. The average of the above ratios is 3.4, but there is a spread of values due to the assumptions of the Galactic models and to the variability of the measured extinction amongst the Galactic sightlines.

Where does our result for $\kappa_{\rm em}(850\,\mu{\rm m})$ stand relative to those for other environments? The average of the values of $x_{\rm B}$ in Table 2 is comparable to Bianchi et al. (2003) when they studied Barnard 68, a dark cloud in the foreground of the Galactic bulge. They concluded that the most characteristic $\kappa_{\rm em}(850\ \mu{\rm m})/\kappa_{\rm em}(V)$ ratio is 4.0×10^{-5} instead of 1.8×10^{-5} that results from Eq. (5). The study by del Burgo et al. (2003) of high-latitude Galactic interstellar regions at 200 μm led to similar findings. These authors suggested that the large and cold grains (similar in size to the ones we use and of temperature ~14 K) have an increased FIR emissivity by a factor >4. Ossenkopf & Henning (1994) studied the dust emissivity in protostellar cores where grains are often covered with a mantle of ice. They found that at 850 μm the emissivity is about 4–5 times higher than that of the interstellar medium as given by Draine & Lee (1984). In addition to this they presented a less realistic scenario of cores with bare grains (without ice coating), where $\kappa_{\rm em} = 3.5\ {\rm cm^2\ gr^{-1}}$ at 850 μm, for atomic hydrogen density $n_{\rm H} = 10^6\ {\rm cm^{-3}}$. This is an order of magnitude higher than Draine's (2003) value ($\kappa_{\rm em} = 0.382\ {\rm cm^2\ gr^{-1}}$). The crucial question, though, is to what degree emissivities derived from such environments can be used for a spiral galaxy as a whole.

James et al. (2002) calibrated the emission coefficient at 850 μm for a sample that included several types of galaxies and found that $\kappa_{\rm em} = 0.7\ {\rm cm^2\ gr^{-1}}$. The method applied was to express the dust mass in two ways, one in terms of the gas mass and the metallicity, the other in terms of the gray-body emission law, and then to equate the two expressions. Thus, they managed to solve for the emission coefficient independently of the dust mass. Although this is the theoretically optimal treatment, their method assumes that the amount of metals locked up in dust grains is constant for all galaxies. They also rely on the CO to H_2 conversion factor X. Other authors (Dumke et al. 1997) believe that X has so many uncertainties on its own, that it is safer to calibrate its value with the aid of the dust emission. More details on the accuracy of the X factor can be found in Maloney & Black (1988) and Arimoto & Sofue (1996). Nevertheless, James et al. (2002) claim that the uncertainty attached to their result is a factor of 2, in which case it is closer to our result. Dunne et al. (2000) calculated the dust masses for the Scuba Local Universe Galaxy Survey (SLUGS) assuming $\kappa_{\rm em} = 0.77\ {\rm cm^2 gr^{-1}}$, a value very similar to that of James et al. (2002). Recently, Seaquist (2004) found that for a revised conversion factor X, the masses of the SLUGS galaxies have to be reduced by 25–38%, which would lead to a similar increase in their value of $\kappa_{\rm em}$, reducing the difference from our result.

Our calculations for the values of $\kappa_{\rm em}(850\ \mu{\rm m})$ can be directly compared with the studies of Alton et al. (1998) and Alton et al. (2004) where the three galaxies studied here are also included. Although their method is based on simple assumptions (they compare the model derived optical depth with the 850 μm flux density), they derive a value for $\kappa_{\rm em}(850\ \mu{\rm m})$ which is 4 times that of Draine & Lee (1984). This result comes in good agreement with the conclusions of our method, which uses a much more realistic way of calculating the submm emission of the galaxy (by computing the temperature distribution in a self consistent way for every point inside the galaxy, in contrast with the method of Alton et al. (1998) and Alton et al. (2004), where they use simple grey-body fits to derive the dust temperature).

Another recent estimate of the 850 μm emission coefficient in nearby spirals is given in the recent study of Meijerink et al. (2005) on the face-on galaxy M 51. These authors present an 850 μm map of M 51 and estimate that $\kappa_{\rm em}(850\ \mu{\rm m})$ is $1.2\ {\rm cm^2\ gr^{-1}}$ (about two times higher compared with values widely used in the literature) based on a canonical gas-to-dust ratio.

4. Results of the "2-disk" model

Once more, we followed the prescriptions of Sect. 2 to determine the parameters that give the optimal fit to the observational data. Their values for this "2-disk" case are presented in Table 3 and their computed SEDs are shown in Fig. 5 as

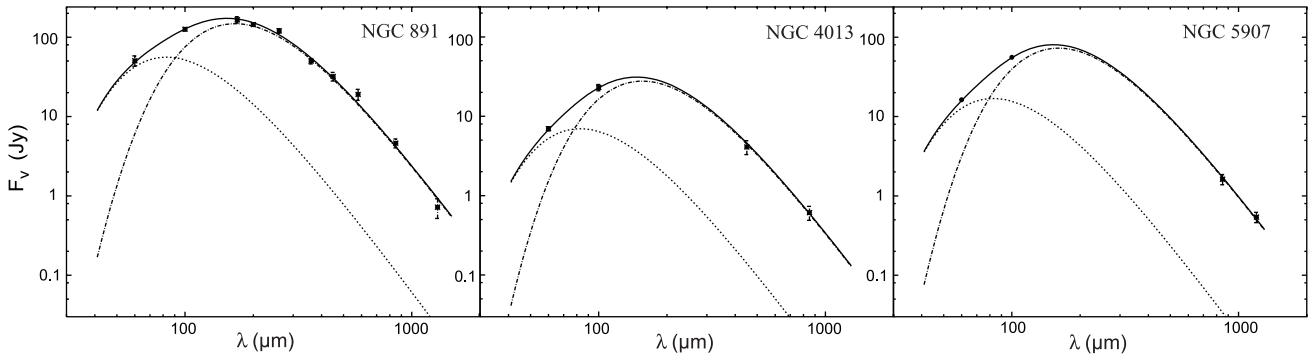

Fig. 4. The observational data of the SED of NGC 891, NGC 4013, and NGC 5907 and our "1-disk" model fits (solid lines) to them. The short-dashed and dashed-dotted lines give the contributions of the HII regions and the diffuse dust respectively.

Table 2. Ratios x_B, x_W, and x_D of our emission coefficient to that of Bianchi et al. (1999), Weingartner & Draine (2001) and Draine (2003), respectively, at 850 μm.

Galaxy	x_B	x_W	x_D
NGC 891	2.3	2.1	2.8
NGC 4013	4.1	3.7	4.9
NGC 5907	3.4	3.0	3.9

Table 3. The best fitting parameters of our "2-disk" model.

Galaxy	*SFR* ($M_\odot$ yr^{-1})	*F*	M_{d1} ($M_\odot$)	M_{d2} ($M_\odot$)
NGC 891	3.40	0.40	5.6×10^7	1.3×10^8
NGC 4013	0.80	0.32	4.5×10^6	1.6×10^7
NGC 5907	2.40	0.26	1.5×10^7	3.5×10^7

solid lines. As in the "1-disk" model, the SEDs fit the observational data very well and do not distinguish between the two possibilities.

From Table 3 we see that we need a total dust mass M_d which is 3.6 times that of the "1-disk" model (on average for the three galaxies), while in Table 2, an enhanced emissivity of about 3.9 times (again on average) that of Draine's model is needed in order to account for the observed flux. This is not an unexpected result. Under the simplifying assumption that the FIR/submm SED can be described by a gray-body law, the quantities M_d and κ_{em} have an inverse proportionality relation for a given 850 μm flux (e.g. Dunne & Eales 2001). In reality, this assumption is only valid for optically thin environments. The optically thicker the environment gets, the more the results deviate from what the above reasoning indicates.

Popescu et al. (2004) found that the second dust disk of NGC 891 contains mass equal to 7×10^7 $M_\odot$ and thus a total dust mass 2 times the value of Xilouris et al. (1999) (instead of 3.4 that we found). This difference may originate from the adopted emission law. Popescu et al. (2004) described the grain emission following the Laor & Draine (1993) recipe while, as already mentioned, we selected the more recent values of Draine (2003).

Except for the total dust mass, a notable parameter now is the SFR, which is approximately half of that needed in the "1-disk" case to provide the required UV radiation to heat the dust. This is reasonable because as the number of emitting particles increases, so does their emitted power, if they are in an optically thin or moderate environment.

5. Comparison between the two models

By either adjusting the dust emissivity or the dust mass we succeed in fitting the FIR/submm SED. In this section we compare the two models.

We start with the submm regime. In Fig. 6 we show the 850 μm theoretical images of the "1-disk" model (top), the "2-disk" model (middle) and the percent difference of the second to the first (bottom). The fractional deviation between the two images is less than 20% throughout the galaxy. Unfortunately, the data is inconclusive because of the poor SCUBA resolution and because of the short spatial extent of the galaxies along the vertical direction.

Nevertheless, the data resolution is sufficient for the comparison of the 850 μm flux radial distribution, along the major axis, with that predicted by our models. Since we know the three dimensional distribution of the emitted power within the galaxy, the radial profiles are easily created by projecting all galactic positions' flux to the central plane. Then, the models are smoothed to the data resolution. The results are given in Fig. 7 (left panels). The solid lines correspond to the "1-disk" model while the dashed ones to the "2-disk" model. Both models provide acceptable fits if one neglects the peculiarities of each individual galaxy which cannot be reproduced by a smooth model. In the same figure, the temperature distribution of the grains is given. Both cases agree with other authors (Dumke et al. 1997; Dunne et al. 2000; Dupac et al. 2003a; Dupac et al. 2003b; Alton et al. 2004).

We compare the NIR appearance of one of the galaxies in our sample (namely NGC 891) when the two different models ("1-" and "2-disk") are considered. The extinction caused by the dust in these wavelengths, and especially in the *K*-band, is low, making any additional dust features easily detected. For NGC 891, the central edge-on optical depth in the *K*-band is $\tau_K^e = 2.7$ (as derived from Xilouris et al. 1999). Thus, a very weak dust lane is seen in the *K*-band image (see the upper panel of our Fig. 8). The "1-disk" model fits very well the *K*-band image of NGC 891 (Xilouris et al. 1998; see also the middle panel of our Fig. 8). The "2-disk" model on the other hand has

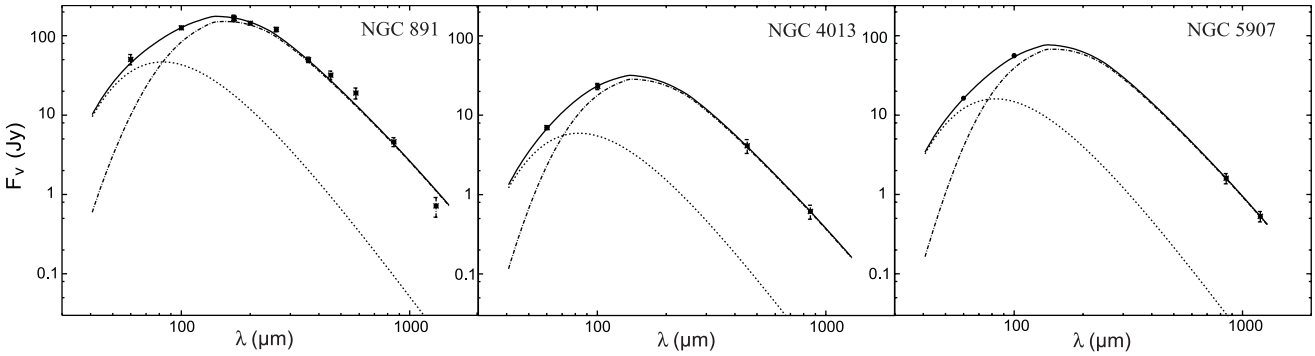

Fig. 5. Same as in Fig. 4, but for our "2-disk" model.

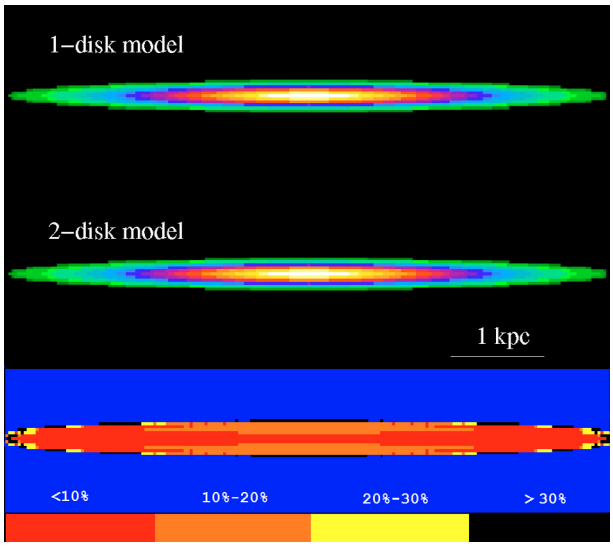

Fig. 6. The "1-disk" and "2-disk" theoretical images (of NGC 5907) at 850 μm and their percentage difference are displayed from top to bottom. The deviation is illustrated by the key at the bottom. It is obvious that in the submm the two model images are very similar to each other.

a central, edge-on optical depth equal to 15.6 in the K-band and creates a very prominent dust lane (Fig. 8, lower panel). Such a high value for τ_K comes from the fact that we have added the contribution of the second, thin, dust disk to that of the first disk to find the total optical depth. Since the second disk has a scaleheight of 90 pc, it is ∼3 times thinner than the first one (Xilouris et al. 1999), contributing significantly to τ_K^e.

A more direct comparison between the two different models ("1-disk" and "2-disk") is presented in Fig. 9. In this plot we show the vertical profile of the K-band image of the galaxy averaged over a region of 430 arcsec along its major axis (stars) together with the vertical profiles of the "1-disk" model (solid line) and the "2-disk" model (dashed line). The region where the profiles are averaged covers most of the galaxy detected in the K-band. This comparison shows the excellent fit of the "1-disk" model (solid line) to the observations; when a second dust disk is included, the dust content is overestimated giving a vertical profile that does not match the data. It is therefore impossible to hide a second dust disk which has comparable or larger dust mass than the first, even if it does not appear in the optical wavebands. Of course, smaller amounts of dust may have gone undetected by our modeling.

The K-band image modeling clearly favors the "1-disk" model. Although we only have K-band data for NGC 891, we have no reason to believe that this is a special case. Thus, our work indicates that the dust emissivity in spiral galaxies at FIR/submm wavelengths seems to be about 3 times what is thought appropriate for the Milky Way.

6. Possible sources of uncertainty

It is important to check whether inaccurate knowledge of certain quantities can lead to different conclusions.

So far we have only considered the possibility that any additional amount of dust (to that in the first disk) lies in a diffuse state (i.e. in a second disk). We also have to investigate the possibility of keeping only the first disk and distributing some extra dust in dense and quiescent clumps. This scenario could be realistic because the clumps do not appear in optical images when not in a high number density. In addition, due to their high concentration of grains, they may contain large amounts of dust and, thus, they may be able to account for the unobserved flux. We will investigate this scenario for clumps of different masses (of order 10^3−10^4 $M_\odot$ and of order $>10^5$ $M_\odot$ respectively).

We argue that it is not reasonable to distribute dust in clouds similar to the dark cloud D of M 17 (as denoted by Dupac et al. 2002), which belongs to the lower mass category. The reason is that the number of clouds needed to reproduce the observed SED renders the galaxy optically thick. In the case of NGC 4013, the emission of the second dust disk is 2.5×10^{42} erg s^{-1}. Presuming that this flux now originates from quiescent clumps, we calculate their number as follows. We fit a gray body of $\beta = 1.9$ and $T = 14$ K to the data of Dupac et al. (2002), as these authors prescribe. This allows us to find the FIR/submm emitted power of the M 17 cloud D, which is equal to 2.8×10^{36} erg s^{-1}. This means that NGC 4013 must have 8.9×10^5 clouds to produce the observed SED. In order to check the effect of such a number of clouds on the optical thickness of NGC 4013, we need a rough estimate of the radius of the M 17 cloud D. From Dupac et al. (2002), it can be inferred to be approximately 10″ or 6.4 pc. When 8.9×10^5 clouds of this radius are uniformly spread on the galactic plane (one next to the other), they form an optically thick disk of radius 6 kpc. For NGC 4013 this corresponds to $\sim 3 r_s$, extending almost to

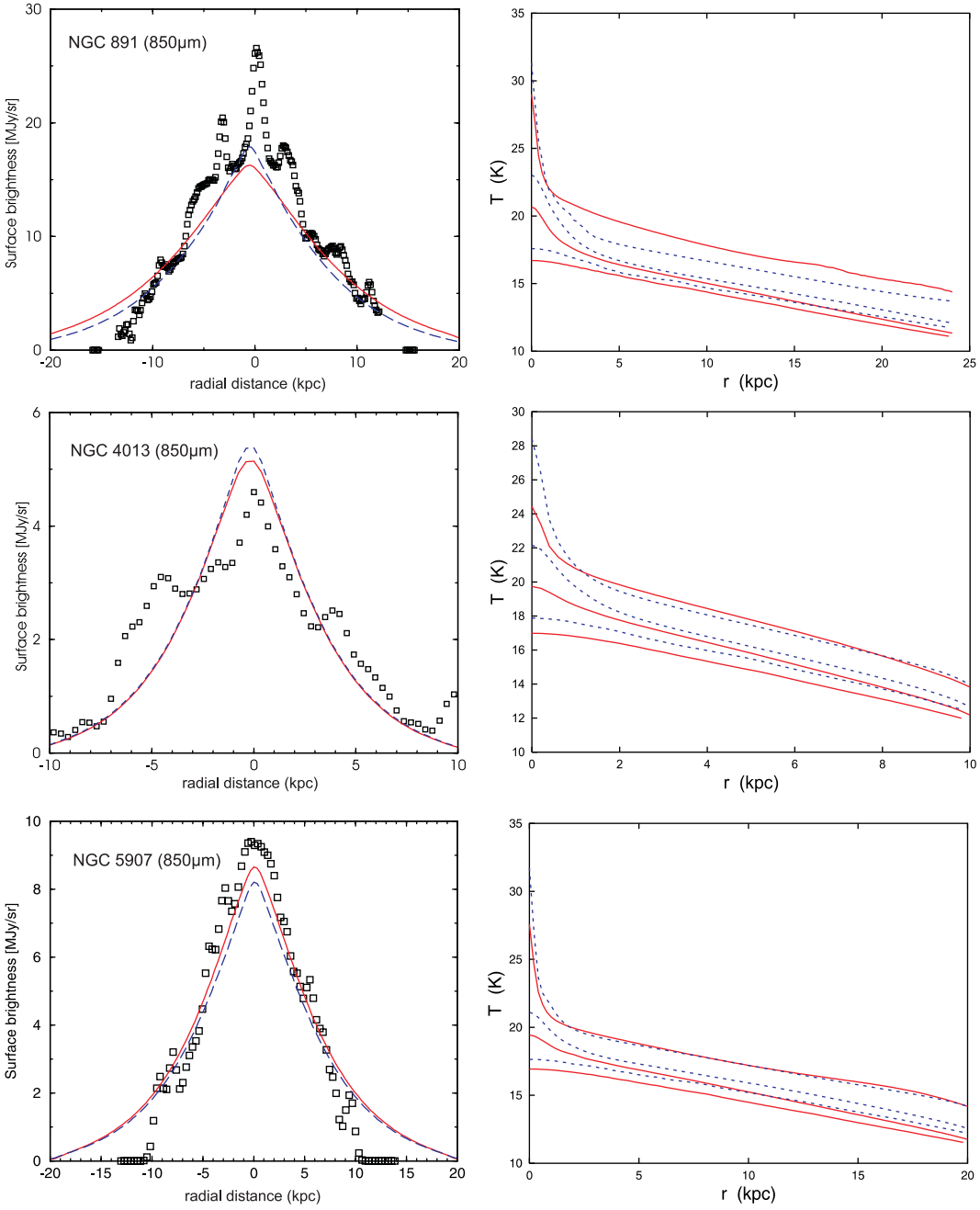

Fig. 7. Flux radial profiles and temperature radial distribution for NGC 891, NGC 4013, and NGC 5907. The solid and the dashed lines correspond to the "1-disk" and the "2-disk" models respectively. The temperature profiles of both models are plotted for several galactic heights, namely, z = 0, 400, and 1600 pc for NGC 4013 and z = 0, 600, and 2400 pc for NGC 891 and NGC 5907 from top to bottom.

the edge of the (baryonic component of the) galaxy and, thus, renders the galaxy opaque. Similarly to the diffuse case, the addition of dust has to be so high that it will inevitably appear in the optical or NIR images.

Clumps of larger size and mass (probably associated with Giant Molecular Clouds) and their effects on the optical thickness of spiral galaxies have been treated in a more sophisticated manner by Misiriotis & Bianchi (2002). These authors showed that clumping can lead to an underestimate of the dust mass by 40% at most. In Sect. 4 we showed that the mass addition necessary to reproduce the observed SED is ~300%. Thus, these clumps only contain a very small fraction of the required dust mass. On the other hand, due to their lower temperatures, they will primarily emit in the submm. Thus, the question is to what degree will their contribution lower the value of $\kappa_{\rm em}$ that we find for the diffuse dust. To answer that, we intend to implement radiative transfer models that take into account clumpiness.

A second source of uncertainty is the value of the quantity β in the emission law (Eq. (6)). The average temperature of the dust in the galaxies of our sample is 16.5 K in the "1-disk" model. According to Dupac et al. (2003b), the appropriate value of β for this temperature is 1.9 rather than 2. If this is the case, the optimal $\kappa_{\rm em}$ of NGC 4013 corresponds to

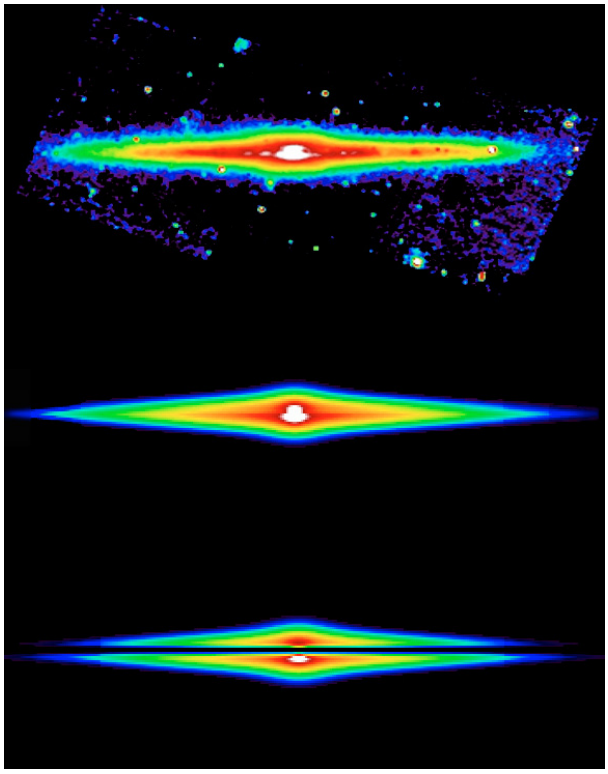

Fig. 8. *K*-band image of NGC 891 (*upper panel*), "1-disk" model (*middle panel*), and "2-disk" model (*lower panel*). The predicted images have been smoothed according to the seeing conditions of the dataset.

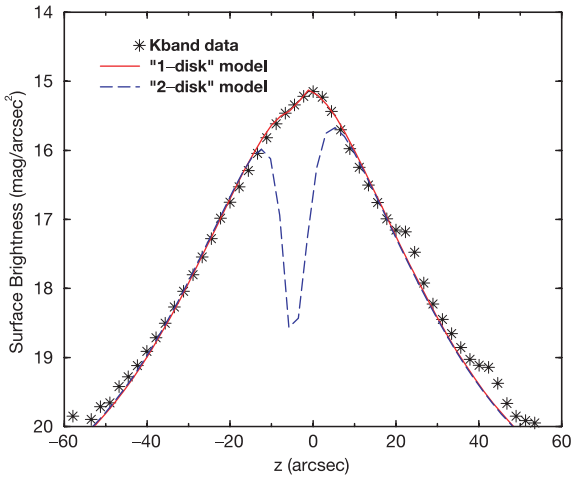

Fig. 9. The vertical profile of the *K*-band image of the galaxy averaged over a region of 430 arcsec along its major axis (stars). This region covers most of the galaxy detected in the *K*-band. Along with the data we present vertical profiles of the "1-disk" model (solid line) and the "2-disk" model (dashed line).

$C_0 = 236$, while the value of the parameters $SFR = 1.77\ M_\odot\,\mathrm{yr}^{-1}$ and $F = 0.17$ remain the same. This results in ratios $x_\mathrm{B} = 4.0$ and $x_\mathrm{D} = 4.8$, which differ very little from the values given in Table 2. In this case, the total SED for NGC 4013 (the SED of both the diffuse dust and the HII region components) is given in Fig. 10 (left panel, dashed-dotted line).

Now we turn our attention to the emissivity at 100 μm. Our average best fit parameters for the $\beta = 2$ law result in a very high value of the emission coefficient at 100 μm. Indeed, in that regime the dust emission is considered to be more accurately described by a $\beta = 1.5$ law. For this reason we also use Eq. (6) with this new value for β and we find that the best fit is depicted in the values $C_0 = 645$, $SFR = 1.70\ M_\odot\,\mathrm{yr}^{-1}$ and $F = 0.13$. The ratios x_B and x_D are now equal to 3.4 and 4.1 respectively. The best fit is again given in the left panel of Fig. 10 (short-dashed line). Our conclusion is that changing the value of β to 1.5 does not have a significant impact on our results.

Since both values of β for our FIR and submm boundary conditions (100 μm and 850 μm respectively) lead to a similar value of $\kappa_\mathrm{em}(850\ \mu\mathrm{m})$, our results are proven to be robust. We are also confident that any other emission law of variable β that complies with these boundary conditions (like that of Reach et al. 1995) will lead to similar findings for the 850 μm emission coefficient. We still prefer to use a constant β model because it has the advantage of being simple.

Two other concerns are the possible contamination of the FIR data from molecular line emission and the effects of VSG. We start with the ^{12}CO $J = 3{-}2$ emission since it contributes to the 850 μm flux, from which we derive our conclusions. Papadopoulos & Allen (2000) found that it accounts for 40% of the total emission in the starburst galaxy NGC 7469. Of course, it has to be much smaller for a quiescent spiral. Dumke et al. (2001) mapped the ^{12}CO $J = 3{-}2$ emission for different types of nearby galaxies and found that the total emitted power in this transition is 2.5×10^{38} erg s^{-1} for NGC 891. This accounts for 1.2% of the flux we used at 850 μm, but it is only a lower limit because the ^{12}CO $J = 3{-}2$ mapping did not cover the whole area of emission. Dumke et al. (2001) argue that the unobserved flux is less than a few percent of the total. Meijerink et al. (2005) who studied the submm emission in M 51 discussed that the molecular contamination at 850 μm is at most 35% in the spiral arms and approximately (less than) 12% for a homogeneous dust disk in the inter-arm regions. We use the average value, 24%, which is close to that of Alton et al. (2004) (20%). At 450 μm, Papadopoulos & Allen (2000) claim that the molecular contribution that comes from the ^{13}CO $J = 6{-}5$ line represents less than 2% of the total flux in a starburst environment. On the other hand, Alton et al. (2004) give an approximate correction of 10% at 450 μm, which is the one we use. The correction of the ISO data for the VSG emission comes from the same source (Alton et al. 2004), is 62% at 60 μm and 14% at 100 μm, and is believed to be somewhat overestimated. Conclusively, we correct the 60, 100, 450, and 850 μm fluxes for our galaxies by reducing them by 62%, 14%, 10%, and 24% respectively. The best fit for NGC 4013 is given in Fig. 10, right panel. The parameters now are $SFR = 1.6\ M_\odot\,\mathrm{yr}^{-1}$, $F = 0.02$, and $C_0 = 262$. The value of C_0 is robust against contamination of our data, and again, our main results are unaffected.

7. Summary and conclusions

We presented detailed modeling of the FIR/submm SED of three edge-on spiral galaxies (NGC 891, NGC 4013, and

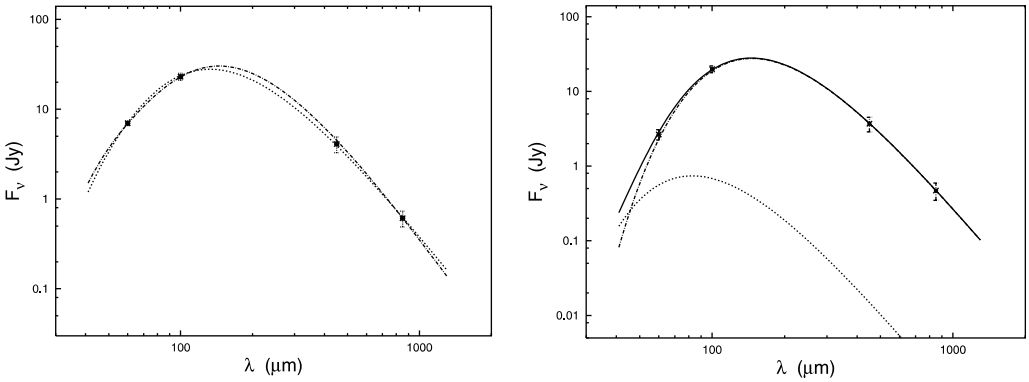

Fig. 10. The left panel is the SED of NGC 4013 for the case of a $\beta = 1.9$ emission law (dashed-dotted line) and for the case of $\beta = 1.5$ (short-dashed line). For the sake of clarity, we plot in this panel the total emission (diffuse dust and HII regions emission together) for each case. The observational data are the same as those in Fig. 4. The right panel is the SED of the same galaxy plotted together with data corrected for VSG and CO emission. This panel is similar to those in Fig. 3 (HII regions, diffuse dust and total emission are plotted in short-dashed, dashed-dotted and solid line respectively).

NGC 5907). We demonstrated that the observed SED can be fitted equally well by a "1-disk" model, where the dust (having a submm emissivity ∼3 times the value widely used in the Galaxy) is distributed in a single exponential disk, or by a "2-disk" model where additional dust (∼2 times more) is distributed in a second thinner disk associated with the young stellar population in spiral galaxies.

The FIR/submm spectrum of spiral galaxies was not able to distinguish between the two models. We showed however, that the "2-disk" model is unrealistic due to its intense dust lane in the *K* band, which is not present in the observations.

Future research on the dust distribution within galaxies (e.g. including more realistic cases like spiral arms, dust clumps, etc.) has to be conducted on both edge-on and face-on systems in order to investigate the existence of more dust hidden within the galaxies and, thus, obtain a better estimate of the properties of the dust grains.

Acknowledgements. We are indebted to D. Lutz for critical suggestions and L. Tacconi, R. Davies for stimulating discussions. Special thanks are owed to the referee, S. Bianchi, for his suggestions and comments that improved our paper significantly. Our work was realized with the aid of the JCMT SCUBA archival data.

References

Alton, P. B., Bianchi, S., Rand, R. J., et al. 1998, ApJ, 507, 125
Alton, P. B., Xilouris, E. M., Misiriotis, A., Dasyra, K. M., & Dumke, M. 2004, A&A, 425, 109
Arimoto, N., & Sofue, Y. 1996, PASJ, 48, 275
Bianchi, S., Davies, J. I., & Alton, P. B. 1999, A&A, 344, L1
Bianchi, S., Davies, J. I., & Alton, P. B. 2000, A&A, 359, 65
Bianchi, S., Goncalves, J., Albrecht, M., et al. 2003, A&A, 399, 43
Cambrésy, L., Jarrett, T. H., & Beichman, C. A. 2005 [arXiv:astro-ph/0501444]
Chini, R., Kreysa, E., Mezger, P. G., & Gemund, H. P. 1986, A&A, 154, L8
de Vaucouleurs, G. 1953, MNRAS, 113, 134
del Burgo, C., Laureijs, R. J., Ábrahám, P., & Kiss, Cs 2003, MNRAS, 346, 403
Draine, B. T., & Lee, H. 1984, ApJ, 285, 89
Draine, B. T. 2003, ARA&A, 41, 241
Dumke, M., Braine, J., Krause, M., et al. 1997, A&A, 325, 124
Dumke, M., Nieten, C., Thuma, G., Wielebinski, R., & Walsh, W. 2001, A&A, 373, 853
Dunne, L., Eales, S., Edmunds, M., et al. 2000, MNRAS, 315, 115
Dunne, L., & Eales, S. A. 2001, MNRAS, 327, 697
Dupac, X., Giard, M., Bernard, J. P., et al. 2002, A&A, 392, 691
Dupac, X., del Burgo, C., Bernard, J. P., et al. 2003a, MNRAS, 344, 105
Dupac, X., Bernard, J. P., Boudet, N., et al. 2003b, A&A, 404, L11
Guélin, M., Zylka, R., Mezger, P. G., et al. 1993, A&A, 279, 37
Hughes, D., Dunlop, J., & Rawlings, S. 1997, MNRAS, 289, 766
James, A., Dunne, L., Eales, S., & Edmunds, M. G. 2002, MNRAS, 335, 753
Kennicutt, R. C. 1998, ARA&A, 36, 189
Laor, A., & Draine, B. T. 1993, ApJ, 402, 441
Lutz, D., Feuchtgruber, H., Genzel, R., et al., A&A, 315, L269
Maloney, P., & Black, J. H. 1988, ApJ, 325, 389
Meijerink, R., Tilanus, R. P. J., Dullamond, C. P., Israel, F. P., & van der Werf, P. P. 2005, A&A, 430, 427
Mihalas, D., & Binney, J. 1981, Galactic Astronomy: Structure and Kinematics (San Francisco: W. H. Freeman and Co.)
Misiriotis, A., Popescu, C., Tuffs., R., & Kylafis, N. D. 2001, A&A, 372, 775
Misiriotis, A., & Bianchi, S. 2002, A&A, 384, 866
Ossenkopf, V., & Henning, T. 1994, A&A, 291, 943
Papadopoulos, P. P., & Allen, M. L. 2000, ApJ, 537, 631
Popescu, C. C., Misiriotis, A., Kylafis, N. D., Tuffs, R. J., & Fischera, J. 2000, A&A, 362, 138
Popescu, C. C., Tuffs, R. J. A., Kylafis, N. D., & Madore, B. F. 2004, A&A, 414, 45
Reach W. T., Dwek, E., Fixsen, D. J., et al. 1995, ApJ, 451, 188
Seaquist, E., Yao, L., Dunne, L., & Cameron, H. 2004, MNRAS, 349, 1428
Soifer, B. T., Boehmer, L., Neugebauer, G., & Sanders, B. 1989, AJ, 98, 766
Weingartner, J. C., & Draine, B. T. 2001, ApJ, 548, 296
Whittet, D. C. B. 1992, Dust in the Galactic Environment (Bristol: Institute of Physics Publishing)
Xilouris, E. M., Kylafis, N. D., Papamastorakis, J., Paleologou, E. V., & Haerendel, G. 1997, A&A, 325, 135
Xilouris, E. M., Alton, P. B., Davies, J. I., et al. 1998, A&A, 331, 894
Xilouris, E., Byun, Y., Kylafis, N., Paleologou, E., & Papamastorakis, J. 1999, A&A, 344, 868